Vesicle cylinders in vapor-differentiated basalt flows

Fraser Goff

Earth and Environmental Sciences Division, Los Alamos National Laboratory, Los Alamos, NM 87545, USA

Abstract

Vesicle cylinders are vertical pipes filled with bubbles and residual melt that differentiate from diktytaxitic basalt flows during crystallization. They grow from about 0.25 m above the base of the flow to the bottom of the chilled flow top. Field relations limit their growth to the period between cessation of lava movement and deep penetration of columnar joints. Basalts containing vesicle cylinders show positive correlations among increasing cylinder abundance, increasing lava porosity, and increasing groundmass crystal size. These features suggest unusually high water contents in the magma before eruption. Although both vesicle cylinders and host lava are "basaltic", the cylinders are enriched in elements not removed by the initial crystallization of the host: Fe, Mn, Ti, Na, K, P and many incompatible trace elements. The last residues to solidify within the cylinders consist of dacitic-rhyolitic glass, Fe-Ti oxides, anorthoclase, apatite ± fayalite ± aegerine. Geothermometry indicates that the cylinders began forming at ~ 1100–$1075°C$ but ceased crystallizing at $\sim 950°C$. Pre-eruptive, high-temperature, iddingsite alteration of olivine phenocrysts in many lavas containing vesicle cylinders shows that the f_{O_2} of the magmas was extremely high at eruption ($\sim 10^{-4}$). After eruption, the f_{O_2} of the lavas fell dramatically to values of about 10^{-11} and conditions paralleled the FMQ buffer to final crystallization. Because the iddingsite forms before eruption, the magmas may become relatively oxidizing by addition of meteoric water late in their evolution. Oxygen-18 analyses of four basalt-differentiate pairs suggest that meteoric water addition has occurred in some of the magmas. Field relations and thermal profiles of cooling lava flows limit the growth period of vesicle cylinders to 1–5 days after flows of typical thickness (3–10 m) come to rest. Estimated viscosities of host lavas and frothy differentiate during cylinder growth are $\leq 10^6$ and $\sim 10^4$ poise, respectively. Although an adequate quantitative model describing growth of vesicle cylinders does not exist, they apparently form by bubble nucleation and resulting density instability above the rising lower solidification front of the cooling flows. As the coalesced bubbles rise, residual melt and additional vapor migrate into the low-pressure, vertical discontinuity formed by the plume.

1. Introduction

Basaltic lavas, lava lakes, sills and layered gabbros produce a variety of tubes, veinlets, pods and layers of differentiated materials that evolve in-situ from the parent magmas by fractional crystallization (i.e., Bowen, 1928; Walker, 1956; Wager, 1960; Murata and Richter, 1961; Kuno, 1965; Anderson and Gottfried, 1971; Anderson et al., 1984; Helz,

1980, 1987; Hon et al., 1994). Perhaps the most spectacular example of these phenomena in basalt flows is the growth of vesicle cylinders and vesicle sheets (segregation pipes, segregation veins). These differentiated structures extend throughout the host lava and contain a continuum of fractionated compositions (Goff, 1977). Basaltic host to rhyolitic residuum can coexist in small hand samples of the cylinders.

Kuno (1965, p. 307) first described vesicle cylinders in the Warner Basalt of northeastern California. A.T. Anderson and colleagues have described many differentiated materials formed in the vesicle-cylinder-bearing Hat Creek Basalt, also of northeastern California (Anderson, 1971; Goff, 1995). Although excellent examples are relatively rare, vesicle cylinders may be found in alkali and tholeiitic lavas of any geologic age or tectonic setting (Table 1; Fig. 1). The author has studied vesicle cylinders in basalt flows of Miocene to Quaternary age throughout the United States (Goff, 1977) and has observed them in the Quaternary Auckland volcanic field of New Zealand. Vesicle cylinders are also found in the Precambrian Keweenawan Basalts of Michigan (Cornwall, 1951) and the Columbia River Basalt of Washington (Table 1). They are found in alkali and tholeiitic basalts of Miocene to Quaternary age in Arizona and New Mexico (e.g., Hiza, 1988). However, as early descriptions indicate, vesicle cylinders are particularly abundant in some Plio-Pleistocene high-alumina basalts of the eastern Cascade Range and the Modoc Plateau of Washington, Oregon and California.

Although Kuno recognized the cylinders as differentiates of host basalt, he offered no explanation for the process that formed them. Goff (1977) noted that all flows containing vesicle cylinders have dikty-taxitic texture. He also observed that the cylinders form at regularly spaced intervals and that their high vesicularity causes them to rise as low-density plumes that feed a network of overlying sheets. Anderson et al. (1984) proposed that differentiated liquids flow from host basalt into segregation structures by gas filter-pressing. Manga and Stone (1994) suggested that the cylinders evolve from bubble aggregates nucleating above the lower solidification front in the lavas (McMillan et al., 1989).

The object of this paper is to document field descriptions, physical properties and geochemical characteristics of vesicle cylinders and their host basalts, and to discuss some requirements for cylin-

Table 1

Locations of some basalt flows containing examples of vesicle cylinders, sheets and pods

Map No.	Name	Age	Type [a]	Location
1	Togiak	Pleis.	A	exposed along beach, east side of Togiak Bay, AK; 59°N, 160°50′W
2	Museum (CRB) [b]	Miocene	T	southbound lane, Interstate 90, 6 km north of Vantage, WA
3	Underwood	Pleis.	HAT	cliff face about 60 m above Highway 30, 3 km west of Bingen, WA
4	Crag Rat	Pleis.	HAT	west Hood River interchange, Interstate 80N, Hood River, OR
5	Panorama Point	Pleis.	HAT	roadcut along east side, Highway 85, 3.3 km south-southeast of Hood River, OR
6	Bend	Pleis.	HAT	junction of Highways 97 and Business 97, north of Bend, OR
7	Warner	Pliocene	HAT	south side of Highway 395, 6 km northeast of Alturas, CA
8	Warner	Pliocene	HAT	top of grade, west side of Highway 139, 8 km northwest of Canby, CA
9	Petroglyph	Pliocene	HAT	upper Petroglyph Canyon; NE1/4, NW1/4, Sec.9, T22S, R40E, Coso Peak Quad., CA
10	Albuquerque	Pleis.	T	Unser Street, Petroglyph National Monument, Albuquerque, NM
11	Cerro Verde	Pleis.	T	upper cliff face, south side of Rio San Jose, 6.7 km southeast of Suwanee, Highway 6, NM
12	Afton	Pleis.	A	upper flow unit of flows exposed inside Kilbourne Hole, south-southwest of Las Cruces, NM

[a] A = alkalic basalt; T = tholeiitic basalt; HAT = high-alumina, tholeiitic basalt.
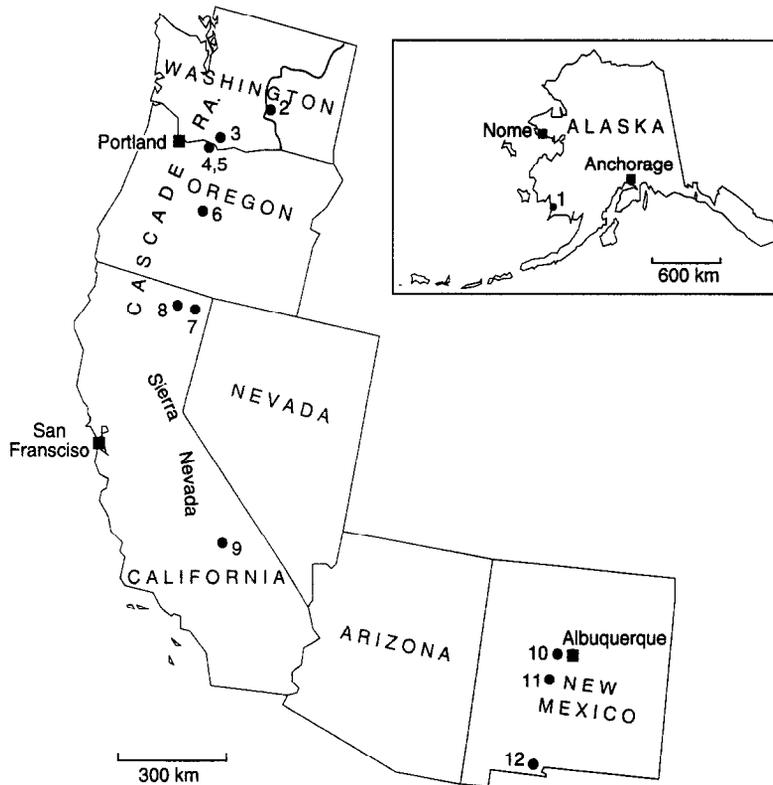[b] CRB = Columbia River Basalt Group.

Fig. 1. Map showing approximate locations of the twelve vesicle-cylinder-bearing flows described in Table 1.

der formation. The data and observations should be sufficient to develop a quantitative model explaining their physical growth. However, the observations also argue that vesicle-cylinder-bearing lavas originate from basaltic magmas unusually rich in water. Determination of the source of that water (shallow or deep) is not resolved although the data presented herein suggest a shallow origin for the water in some of the magmas.

2. Field relations

All flows containing vesicle cylinders that have been studied by the author are pahoe-hoe lavas containing many features indicative of relatively low viscosity conditions. An idealized cross section of a basalt flow containing vesicle cylinders, sheets and pods appears in Fig. 2 whereas some outcrop photos occur in Fig. 3. Physical characteristics are listed in Table 2. Cylinders generally begin growth within 0.25 m of the flow base, or at any higher level in the

lower half of the flow (Fig. 3a). In continuous exposures, entire cylinders can be observed extending from positions near the base of the flow to the bottom of the chilled upper crust of the flow. Cylin-
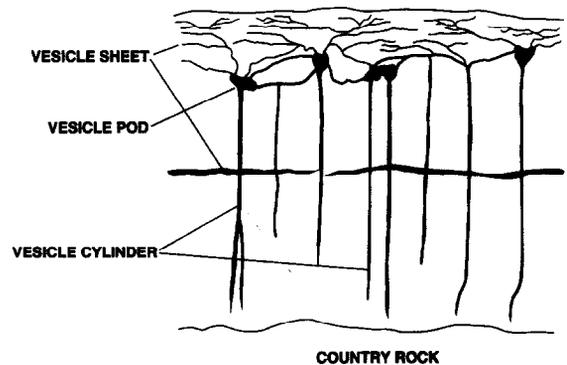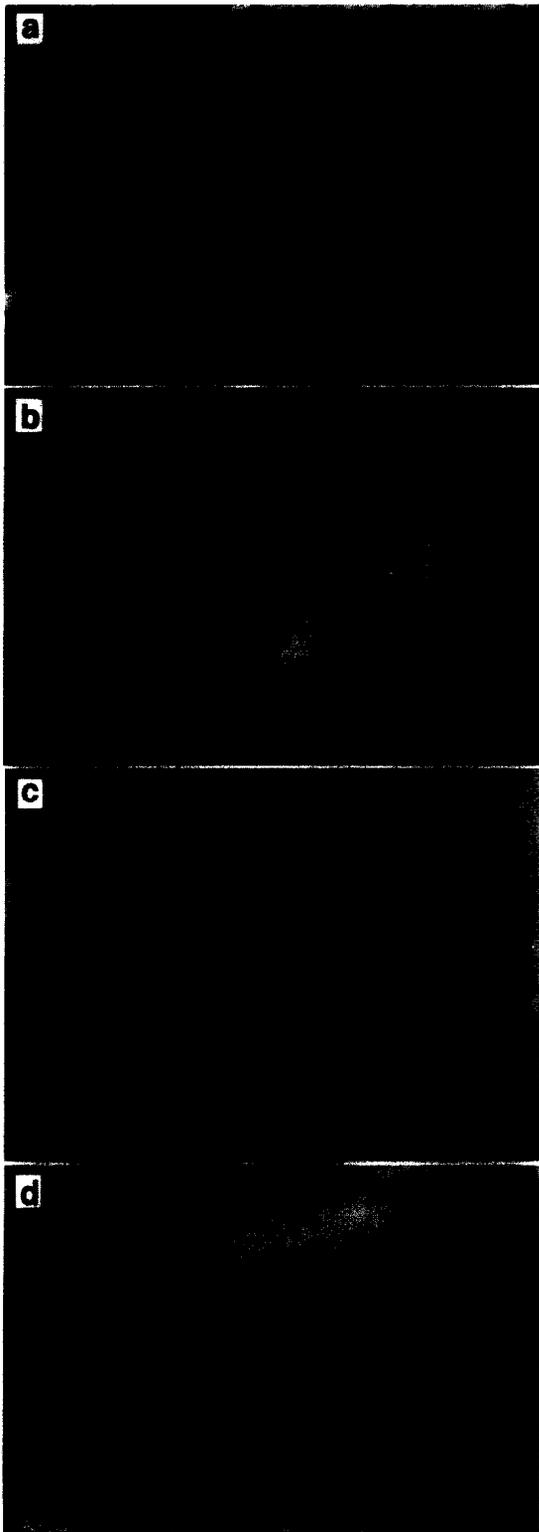

Fig. 2. Idealized cross section of a basalt flow (3–10 m thick) showing the network of vesicle cylinders, sheets and pods. The country rock may be another flow or flow unit of basalt or any other rock type or combination of rock types. Warped cylinders near base of flow indicate that cylinders may form when the flow can still creep.

ders trapped beneath the chilled crust splay into sill-like vesicle sheets (Fig. 3c) or form vesiculated pods of differentiated liquid from which vesicle sheets invade the chilled crust. The cylinders vary from about 2 cm in diameter at their bottoms to as much as 20 cm across at their tops. Vesicle cylinders increase in vesicularity upwards. Most joints cut the cylinders elliptically (Fig. 3a and d). At higher levels in the flow, individual cylinders occasionally merge into single, collective cylinders (Fig. 4a).

On large horizontal surfaces in the lower half of a flow, the cylinders display relatively uniform spacing (Fig. 3b). Such exposures reveal 30 or more vesicle cylinders per square meter, depending on the flow and position of the exposure within the flow. Average closest spacing among cylinders can be < 20 cm.

Rarely, some vesicle cylinders appear to originate from elongated (pipe) vesicles in the quenched bottoms of some flows. However, vesicle cylinders should not be confused with pipe vesicles (Philpotts and Lewis, 1987) which reside at the bottoms of flows and which generally lack differentiate. Vesicle cylinders invariably occur above the zone of pipe vesicles and extend upward to the base of the chilled top crust of the flow.

Because the cylinders are nearly vertical and can be traced vertically for several meters, they can only have formed after the host lava essentially ceased all movement. Occasionally, a region in a flow at a given height (usually near the flow bottom) will contain several cylinders all warped in the same direction (Fig. 2) showing that the cylinders can form while the lava is still plastic enough to creep.

Fig. 3. Photos of vesicle cylinder features. (a) Central section of lava, Basalt of Petroglyph Canyon, Coso volcanic field, California; vertical face on right shows several longitudinal sections of cylinders whereas near-horizontal face on left shows many circular sections (hammer handle is 46 cm long). (b) Large fallen block from Cerro Verde basalt flow, New Mexico showing distribution of vesicle cylinders in horizontal exposure. (c) Vertical joint face in Panorama Point basalt, Oregon showing vesicle cylinder branching into vesicle sheets. Larger vesicles accumulate and flatten at upper contact of sheet. (d) Elliptical cross section of vesicle cylinder about 3 cm long from about 1 m above flow unit base in coarsely porphyritic, diktytaxitic Panorama Point basalt. The visual contrast between host basalt and glassy, bubble-rich differentiate is usually pronounced in fresh exposures.

Table 2
Physical/chemical characteristics of four vesicle-cylinder-bearing, high-alumina tholeiites [a]

Characteristic	Crag Rat	Panorama Point	Warner, Alturas	Warner, Hwy 139
VC/m^2, 1 m above flow base	15	30	20	20
Ave. closest VC spacing 1 m above base (cm)	33	19	26	24
Max. gdmass pheno. dimension, plag (mm)	1.1×0.24	6.4×0.8	1.3×0.24	1.6×0.30
Phenocryst content at eruption (%), vesicle free	≤ 48	≤ 44	≤ 50	≤ 50
Average porosity (%)	7.2	13	12	10
Iddingsite alteration of olivine pheno. (%)	5–8	80–90	30–40	30–40
Thickness of flow (m)	8	6	8	7
Max. height of VC (m)	6–6.5	4–4.5	6–6.5	5.5
Calc. eruption temperature (°C) [b]	1110	1145	1235	1205
Calc. viscosity of differentiate (poise) [c]	4.2×10^4	1.1×10^4	2.3×10^4	2.3×10^4

[a] Data from Goff (1977); locations in Table 1 and Fig. 1.
[b] From olivine-glass geothermometer of Roeder and Emslie (1970).
[c] From Shaw (1972); assumes temperature of 1075°C, water content of 0.5 wt.%, 40% crystals and 10% bubbles.

Columnar joints always cut vesicle cylinders; cylinders never migrate toward a joint surface and flow up the fracture. Thus, vesicle cylinders finish growth before deep penetration of columnar joints into the flow interior.

Vesicle sheets form an intricate network of sill- or vein-like bodies that increase in complexity upwards until they become indiscernible in the frothy flow top. The thickness of individual sheets decreases upwards from about 10 to 0.5 cm, but the number of sheets increases upwards. The sheets apparently spread along incipient horizontal joints in the chilled top crust and through cracks created after the flow top has solidified. Differentiated liquids may ooze into near-surface fractures (Anderson, 1971). Columnar joints of the entablature always cut deeper vesicle sheets.

The relation between cylinders and sheets may be very complicated in individual outcrops because, as the flow top solidifies downwards, new sheets develop that entangle with previously formed cylinders and sheets. Thus, a region of the upper half of some flows contains an interconnecting, cross-cutting network of cylinders, sheets and pods so complex that the mechanism of growth is disguised.

If the vesicle-cylinder-bearing flows are thicker than about 3 m, a central vesicle sheet 10 to 40 cm thick usually forms where the columnar joints growing from the top-down meet those growing from the bottom-up (Murata and Richter, 1961). This sheet is always the last body of differentiated liquid to form in the flow and will nearly always be the thickest

sheet to form. The central sheet cuts and often plastically deforms the vesicle cylinders that grew before it. Thus, this central sheet does not necessarily extract differentiate from the cylinders. In addition, many flows containing a central vesicle sheet do not contain vesicle cylinders.

The boundaries between cylinders and host basalt are generally sharp (Fig. 3d) but basalt crystallizing next to vesicle cylinders is commonly drained of residual liquid. A ring of vesicles may line the perimeter of the cylinders (Fig. 5). Phenocrysts and chunks of host basalt are usually engulfed by the cylinders as they propagate upwards (Fig. 5a). The random vertical distribution of these basaltic fragments suggests that upward flowage was at a rate equal to or greater than gravity settling (see below).

The boundaries between vesicle sheets and host basalt are always sharp (Fig. 4b). Pieces of basalt are often stoped into sheets. The upper interface of the sheets is usually crowded with horizontally flattened vesicles (Fig. 3c) and the lower levels of the sheets sometimes exhibit layers of gravity settled host basalt phenocrysts (Fig. 4b).

3. Petrology of lavas, iddingsite and differentiates

3.1. Lavas

Vesicle-cylinder-bearing lavas invariably have porous diktytaxitic textures (Figs. 4 and 5) that attest to the expansion of the intimate mixture of crystals
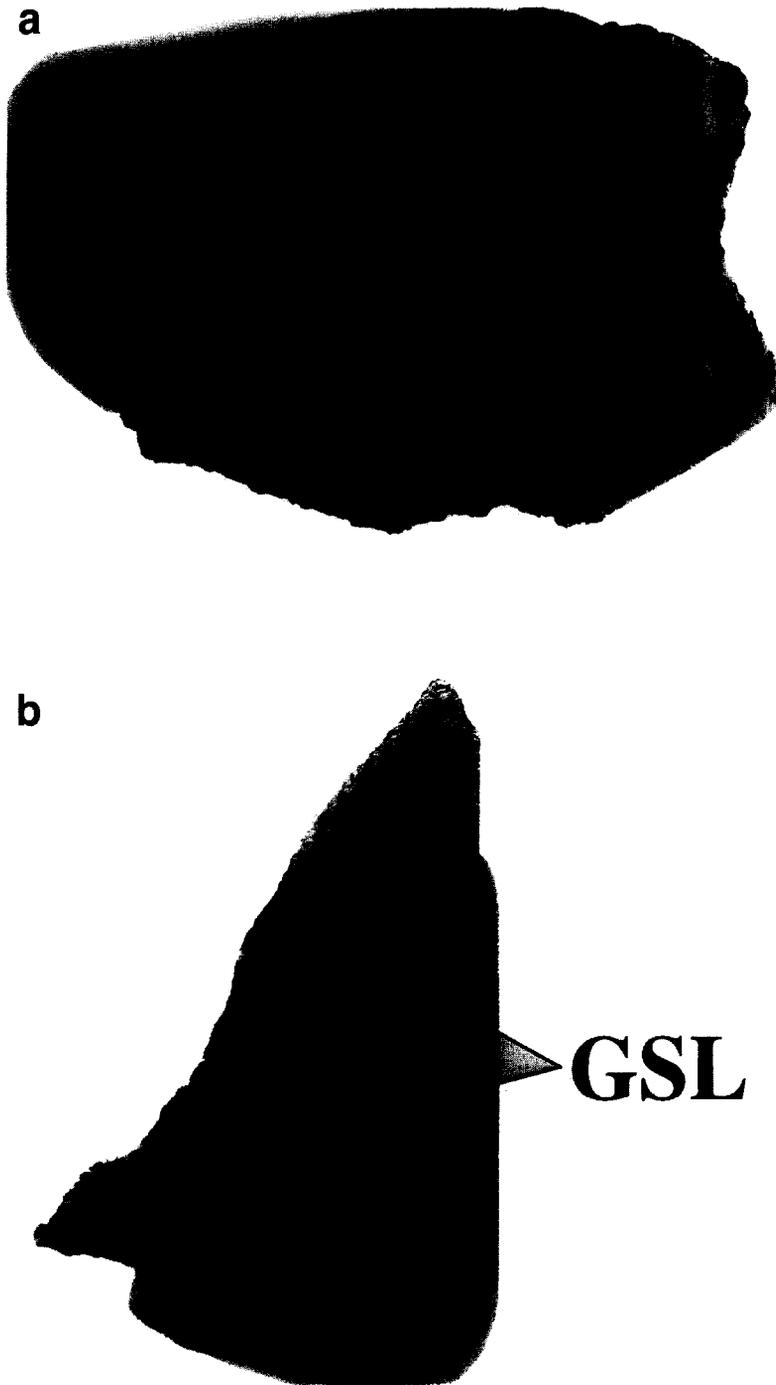
Fig. 4. Photos of cut surfaces through samples of Panorama Point basalt, Oregon. (a) Horizontal cut showing four vesicle cylinders merging into one collective cylinder from upper half of flow unit (all flow units have vesicle cylinders). (b) Vertical cut showing vesicle sheet from upper half of flow unit. The sheet is about 8 cm thick and has a layer of gravity settled olivine and plagioclase (GSL) at the bottom. Vesicles are more abundant above the gravity settled layer and most abundant at the upper contact. Analysis PP3S (Table 4) is from the glassy material above the gravity settled layer.

and melt by water vapor during final stages of crystallization (Fuller, 1931). As a result, average porosities of the flow interiors are high (up to 13%) and bulk densities are low (Table 2). Flows containing vesicle cylinders studied by the author do not display any significant layering of early phenocryst phases formed by gravity settling (Goff, 1977).

High-alumina tholeiites, which predominate in this study, are aphyric to coarsely porphyritic rocks with phenocrysts of olivine and plagioclase in a subophitic matrix of augite, plagioclase, olivine, Fe-Ti oxides, apatite and minor glass (Table 3). The Crag Rat flow contains minor pigeonite. Alkali basalts of this study are similar in appearance to the high-alumina basalts although they may contain some clinopyroxene phenocrysts. Groundmass pyroxene is usually titanium-rich. Tholeiites of the Columbia River Basalt which contain vesicle cylinders are aphyric rocks with rare plagioclase and little or no olivine and pyroxene phenocrysts. Groundmass phases consist of plagioclase, augite, and Fe-Ti oxides in a glassy, sub-ophitic matrix.

3.2. Iddingsite

Well-developed, orange-red iddingsite alteration of olivine phenocrysts is present to pervasive in many lavas hosting vesicle cylinders (Table 2; Fig. 6). Alteration affects the perimeters, cracks and fractures of the crystals but fresh olivine, Fo_{88-80}, remains inside. The altered phenocrysts are rimmed with fresh overgrowths of fayalitic olivine (Fig. 6b). Tiny unaltered fayalitic olivine crystals (Fo_{65-28}), similar in composition to the phenocryst overgrowths, are distributed throughout the groundmass. Thin sections of chilled flow crusts, however, contain olivine with iddingsite, but reveal no fresh fayalitic overgrowths over the iddingsite (Fig. 6a). If we assume that the chilled crust represents the phenocryst assemblage of the lava on eruption, then we can conclude that: (1) the fayalitic overgrowths formed after eruption; and (2) the iddingsite formed at magmatic temperatures before eruption, either in the magma chamber or in the vent as the magma rose. Similar iddingsite textures have been described

Table 3
Compositional range of minerals in four high-alumina tholeiites that form vesicle cylinders, sheets and pods [a]

Pre-eruption phenocrysts and iddingsite	
Olivine:	Fo_{88-72}; contain Mg-rich chromite
Plagioclase:	An_{82-60}
Iddingsite [b]:	Mixture of orthopyroxene, γ-Fe_2O_3, α-Fe_2O_3, cristobalite, amorphous silica and $Fe_2O_3 \cdot H_2O$ (?)
Post-eruption groundmass crystals	
Olivine:	Fo_{65-28}
Plagioclase:	An_{70-30}
Pyroxene:	$En_{45}Fs_{11}Wo_{44}$–$En_{29}Fs_{31}Wo_{40}$; Crag Rat flow has some pigeonite $En_{45}Fs_{50}Wo_5$
Fe-Ti oxides:	$\sim$ 80% ulvospinel; $\sim$ 5% R_2O_3
Differentiated minerals	
Fayalite:	Fo_{25-8}
Plagioclase:	An_{35-5}
Alkali feldspar:	Or_{46-5}
Pyroxene:	$En_{40}Fs_{20}Wo_{40}$–$En_{15}Fs_{42}Wo_{43}$; Crag Rat flow has subcalcic augite $En_{30}Fs_{39}Wo_{31}$–$En_{40}Fs_{52}Wo_8$
Aegerine:	$\leq$ 29 wt.% FeO_T; $\leq$ 10 wt.% Na_2O; found in Warner flows only
Fe-Ti oxides:	62–79% ulvospinel; 4–10% R_2O_3
Vapor-phase mineral	
Cristobalite:	$\leq$ 4 wt.% Al_2O_3 + Na_2O; crystals grow on vesicle walls, primarily in differentiated zones

[a] Data compiled from electron microprobe analyses reported in Goff (1977) for flows described in Table 2.
[b] Data from SEM–EDAX photos and analyses and XRD analyses reported in Goff (1977).
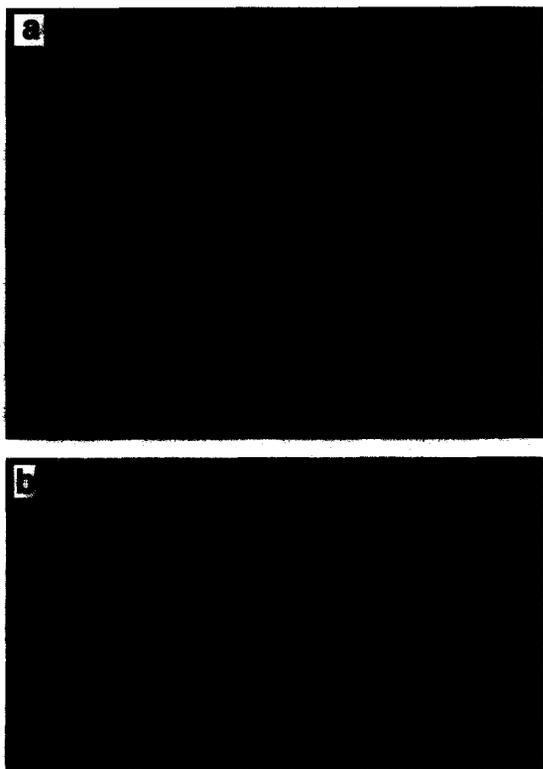
Fig. 5. Photos of very large thin sections showing cylinder textures. (a) Cross section of two merging cylinders about 1 m above base of flow, Crag Rat basalt, Oregon. Clots (C) of groundmass crystals have been engulfed by both cylinders. Larger vesicles accumulate at cylinder margins. Diameter of larger cylinder is about 2 cm. (b) Cross section of cylinder 1.75 cm long about 0.4 m above base of flow unit in Panorama Point basalt (sample PP1dC, Table 4). Bubbles outline the shape of the cylinder forming in the host basalt. Petrographic examination and comparison with host basalt chemistry shows that very little differentiation has taken place in this lowermost part of the cylinder.

from some basalts in northern Mexico and southern New Mexico (K. Cameron, oral commun.; N. McMillan, oral commun.).

Detailed XRD and SEM analysis of large, severely altered olivines from the Panorama Point basalt shows that the iddingsite is composed of an intimate mixture of orthopyroxene, maghemite (γ-Fe$_2$O$_3$), hematite (α-Fe$_2$O$_3$), cristobalite and amorphous silica (Goff, 1977). These phases are similar to those generated during high-temperature oxidation experiments on olivine (Haggerty and Baker, 1967; Champness, 1970; Goode, 1974).

This high-temperature iddingsite is not present in all basalts having vesicle cylinders. In addition, some cylinder-bearing lavas having this iddingsite display overgrowths of unaltered clinopyroxene rather than fayalitic olivine. However, the three-fold association of diktytaxitic lavas, vesicle cylinders and high-temperature iddingsite is common.

3.3. Differentiates

Vesicle cylinders and sheets may be so vesiculated that porosities exceed 30% but usual values are 10–20%. The differentiates primarily contain sodic plagioclase (An$_{35-5}$), augite, Fe-Ti oxides, apatite and glass in a vesiculated intersertal to sub-ophitic groundmass. Differentiate from the more silicic Crag Rat flow also has sub-calcic augite. Cylinders in high-alumina tholeiite from the Warner Basalt contain augite rimmed with aegerine. The last crystallizing residues contain Mn-rich fayalite needles (Fo$_{25-8}$), tabular anorthoclase ($\leq$ Or$_{46}$), and slender prisms of apatite. Fe-Ti oxides form single grains, dendritic networks and elongate blades. Fine, dust-like particles of Fe-Ti oxides coat elongate fayalite crystals. Spherules of vapor-phase cristobalite containing measurable Al and Na commonly cling to the walls of vesicles (Goff, 1977). Presumably, other vapor-phase minerals such as hematite could form on vesicle walls depending on the original composition of the magma, the amount of differentiation occurring in the cylinders, and the total volatile content of the differentiates.

4. Chemistry and geothermometry of lavas and differentiates

4.1. Chemistry

Nine vesicle-cylinder-bearing basalts from various locations in the western USA contain 47.5–52.6 wt.% SiO$_2$. Host lavas listed in Table 4 do not show significant vertical changes in chemistry. Continuous differentiation of liquids that fill the cylinders and sheets produces compositions progressively enriched relative to host lavas in Fe, Mn, Na, K, Ti and P. SiO$_2$ is usually enriched by as much as 3 wt.% in differentiate samples relative to host. However, a

Table 4
Selected chemical analyses of host basalts, vesicle cylinders and vesicle sheets [a]

Sample:	Crag Rat				Panorama Point				Togiak		Petroglyph [b]		Warner	
	CR-AVE [c]	CR25C	CR20C	CR2S	PP-AVE [d]	PP1dC	PP1kS	PP3S	AH26	AH25S	F76-20	F76-21	139-1	139-1C
Type:	Flow	Cyl.	Cyl.	Sheet	Flow	Cyl.	Sheet	Sheet	Flow	Sheet	Flow	Cyl.	Flow	Cyl.
Major elements (wt.%)														
SiO_2	49.0	47.5	49.2	52.1	47.8	48.1	47.6	48.5	50.9	53.6	49.5	50.0	47.7	49.4
TiO_2	1.28	1.52	2.14	3.48	1.38	1.45	3.26	3.16	2.39	3.42	1.3	1.9	1.12	2.38
Al_2O_3	17.0	13.9	14.1	12.7	16.8	16.3	11.8	11.8	14.8	12.5	16.9	15.5	17.8	13.8
Fe_2O_3	2.72	2.67	3.48	5.83	6.31	5.53	8.60	5.55	2.66	2.71	2.5	6.9	3.72	3.79
FeO	8.32	10.5	10.2	8.74	6.47	7.04	9.12	11.9	8.14	9.87	6.2	3.9	6.39	9.24
MnO	0.17	0.20	0.21	0.22	0.19	0.19	0.27	0.27	0.15	0.18	0.12	0.16	0.16	0.22
MgO	7.53	10.7	7.29	3.40	6.73	6.64	3.78	4.01	7.13	3.28	7.4	5.4	8.68	5.55
CaO	9.89	7.96	9.22	7.17	9.94	9.92	8.47	8.67	8.98	6.33	10.2	10.2	11.2	10.7
Na_2O	2.93	2.59	2.99	3.80	2.91	2.87	3.32	3.40	3.52	4.51	3.5	3.8	2.94	3.84
K_2O	0.47	0.59	0.65	1.33	0.49	0.55	1.00	0.97	0.83	1.77	0.67	0.82	0.26	0.50
P_2O_5	0.20	0.24	0.27	0.57	0.21	0.25	0.44	0.46	0.39	0.93	0.30	0.38	0.16	0.37
$H_2O(+)$	–	0.45	0.12	–	–	–	0.60	0.54	–	–	0.25	0.46	–	–
$H_2O(-)$	0.31	0.33	0.11	0.53	0.57	0.72	1.10	0.87	0.10	0.15	0.21	0.27	0.14	0.19
Total	99.8	99.2	100.0	99.9	99.8	99.6	99.4	100.1	100.0	99.3	99.1	99.7	100.3	100.0
Trace elements (ppm)														
Ba	23	26	0?	28	13	–	1	6	–	–	–	–	–	–
Cl	39	44	56	155	34	–	62	70	–	–	–	–	–	–
Rb	23	30	25	44	24	–	37	40	–	–	–	–	–	–
S	<10	<10	<10	<10	<10	–	<10	<10	–	–	–	–	–	–
Sr	383	301	305	279	381	–	281	307	–	–	–	–	–	–
Y	32	34	36	52	30	–	55	49	–	–	–	–	–	–
Zn	114	142	149	271	94	–	211	203	–	–	–	–	–	–

[a] Analyses by XRF and wet techniques (FeO); methods described in Goff (1977).
[b] "Rapid rock" analyses provided by C.R. Bacon (USGS).
[c] Average of eight whole rock analyses and two trace element analyses.
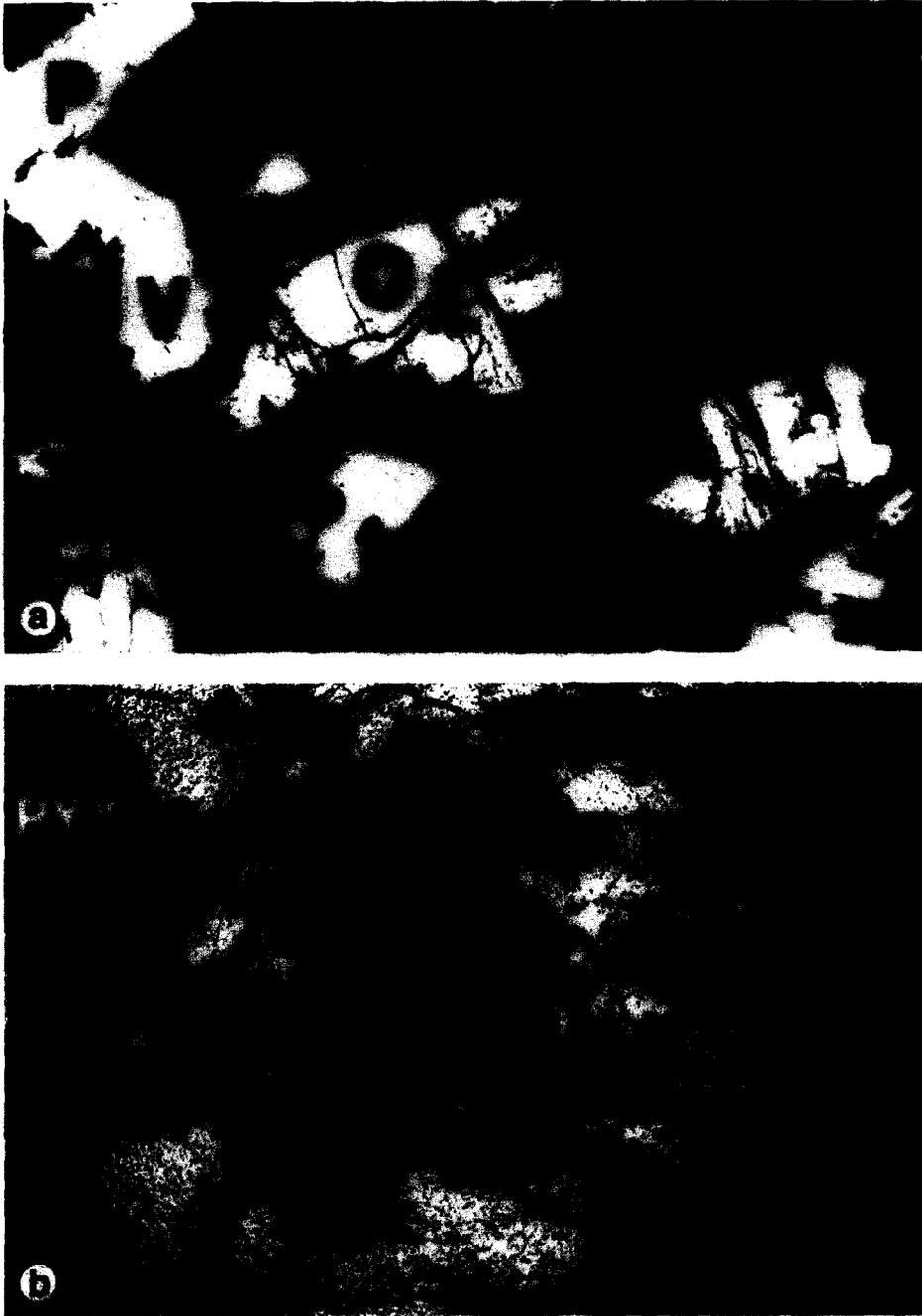[d] Average of two whole rock analyses; one trace element analysis.

Fig. 6. Photomicrographs (transmitted light) of high-temperature, orange-red iddingsite alteration from the Panorama Point basalt, Oregon. Alteration is so extensive that the phenocrysts were used for detailed studies of reaction products described in text. (a) Olivine phenocrysts ≤ 2 mm long with chromite inclusions surrounded by glass, plagioclase and vesicles from chilled pahoe-hoe crust of flow unit. No augite or Fe-Ti oxides have crystallized. Iddingsite alteration is pervasive but no sheath of fresh olivine is present (sample PP1v, Goff, 1977, p. 42). (b) Olivine phenocrysts ≤ 2 mm long from interior of flow have sheath of fresh fayalitic olivine. Similar fayalitic olivine occurs in groundmass. Ophitic augite and Fe-Ti oxides coexist with olivine, plagioclase, vesicles and minor glass. This type of iddingsite forms in the magma chamber or conduit of the chamber before eruption of the lava (F = fayalitic overgrowth and groundmass fayalitic olivine; O = phenocryst olivine; P = plagioclase; PY = pyroxene; V = vesicle).

dramatic decrease is generally seen in Al_2O_3 content (Table 4). Differentiates are also enriched in Cl, Nb, Rb, Y, Zr and Zn (Anderson and Gottfried, 1971; Goff, 1977), elements incompatible with the primary host minerals. Glass compositions from the quenched base of the flows are slightly more silicic than whole rock compositions due to presence of coexisting olivine and plagioclase (i.e., Crag Rat flow, Table 5). Residual glasses in the lavas and differentiates range from basaltic to rhyolitic (≤ 73 wt.%) but the most silicic patches are found in the differentiates (Fig. 7).

Based on Pearce element ratio diagrams (Russell and Stanley, 1990), the chemical variations among host basalt, bulk differentiate and residual glass are explained by a combination of Ol-Plag-Cpx $\pm$ Fe-Ti oxide fractionation (as seen in thin sections). The transition from host to differentiate to residual glass parallels classic crystal fractionation trends on AFM diagrams (Fig. 7). Similar fractionation trends have been previously documented from segregation structures in other lavas (Kuno, 1965; Anderson et al., 1984) and in larger mafic bodies such as lava lakes, sills and layered gabbros (Walker, 1956; Wager, 1960; Murata and Richter, 1961; Helz, 1987; Chapman and Rhodes, 1992). However, in the larger more insulated bodies, slower cooling, convection, and re-equilibration of liquid with gravity settled crystals, particularly olivine, creates more complicated frac-tionation patterns compared to those observed in vesicle cylinders and sheets.

4.2. Geothermometry

Thermometry determined from compositions of minerals and glasses establish: (1) the eruption temperature of the lavas; and (2) the range of temperatures over which vesicle cylinders and their residual components were crystallizing. The eruption temperatures of four different vesicle-cylinder-bearing basalts (Table 2) were estimated at ~ 1110–$1235°C$ using the olivine-glass geothermometer (Roeder and Emslie, 1970). These estimates use average glass compositions determined from the quenched flow tops or flow bottoms such as those in Table 5. Because the olivine phenocrysts immersed in these quenched glasses have high-temperature iddingsite alteration containing Fe_2O_3 phases (Fig. 6a), the f_{O_2} of magmas containing this alteration was about 10^{-4} just before eruption (Fig. 8) when volatile content was highest.

Unoxidized Fe-Ti oxide pairs are difficult to find in the differentiated liquids filling the cylinders. Five pairs from four flows yield a range of temperatures (950–1050°C) and oxygen fugacities ($10^{-13.5}$–10^{-11}; Lindsley and Frost, 1992) that parallel the fayalite-magnetite-quartz buffer (FMQ, Fig. 8). This is not

Table 5
Selected chemical analyses of glasses from the Crag Rat flow [a]

Sample:	Flow [b] CR-AVE	Quenched glasses [c]				Residual glasses [d]					
		CR-35a	CR-35b	CR-35c	CR-35d	CR-27a	CR-25b	CR-2a	CR-29Sc	CR-29Sb	CR-2c
SiO_2	49.0	50.4	52.5	52.1	51.1	64.8	68.5	69.0	70.4	72.3	73.4
TiO_2	1.28	2.28	2.03	1.89	1.98	0.53	0.65	1.67	1.70	0.40	0.43
Al_2O_3	17.0	14.0	17.1	16.8	16.3	19.1	15.8	13.1	12.1	14.6	14.3
Fe_2O_3	2.72	2.57	1.94	2.17	2.35	1.01	1.63	0.82	2.74	1.36	0.44
FeO	8.32	10.6	7.95	8.91	9.63	1.76	2.30	2.97	4.38	2.22	1.59
MnO	0.17	0.13	0.13	0.16	0.13	0.09	0.05	0.08	0.10	0.07	0.04
MgO	7.53	5.22	3.54	4.36	5.00	0.73	0.10	0.56	0.29	0.22	0.29
CaO	9.89	8.25	8.92	8.92	9.86	1.55	0.35	2.68	2.21	0.14	0.16
Na_2O	2.93	3.53	4.50	4.21	4.03	5.29	5.09	3.66	4.57	3.44	4.01
K_2O	0.47	1.04	0.66	0.56	0.72	4.83	4.55	3.90	0.65	6.75	4.66
Total	99.3	98.0	99.3	100.1	101.1	99.7	99.0	98.4	99.1	101.5	99.3

[a] Analyses by electron microprobe using methods described in Goff (1977, appendix II).
[b] Average analysis of eight samples from Table 4.
[c] Analyses from sample collected at quenched base of flow.
[d] Analyses from samples of groundmass lava, vesicle cylinders and vesicle sheets.

unreasonable because the differentiates are crystalliz-
ing fayalitic olivine, ulvospinel and silicic glass while
volatiles degas to form bubbles. The exact tempera-
ture of formation for the cylinders must vary from
flow to flow depending on several factors including
chemical composition, water content, eruption tem-
perature and nucleation rate of bubbles (see below).
An average temperature of formation of 1075°C is
used for the calculations of differentiate viscosity
described below but the cylinders in some flows,
such as the very widespread and hot Warner Basalt,
must form at temperatures above 1100°C. In con-
trast, residual pockets of liquid in the cylinders and
sheets are crystallizing at temperatures below 1000°C.

In a somewhat comparable study, Helz (1980,
1987) described the diverse structures and fractiona-

tion processes developing during crystallization of
basalt in the 1959 Kilauea Iki lava lake. The eruption
temperature of the picritic tholeiite was as high as
1215°C. Helz (1987, p. 253) hypothesized that di-
apiric melt transfer was occurring in the lake and
that this low-density melt was forming at 1145–
1160°C, "at and just below the incoming of plagio-
clase" (the diapirs were not visible in core samples).
Segregation veins in the lava lake are coarse-grained
diabasic sills having liquidus temperatures of 1135–
1105°C. Liquids in segregation veins "start to di-
verge from those in the host at temperatures of"
1085–1070°C. Liquidus temperatures of 1060–
1000°C were determined for the most highly differ-
entiated liquids filling fractures or large vesicles.

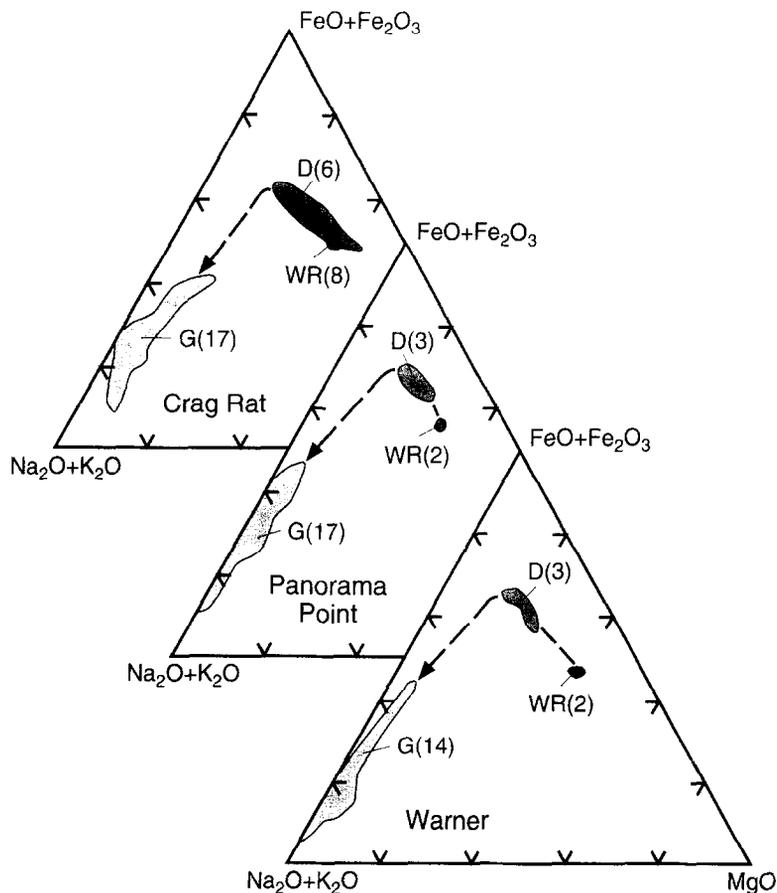Helz and Thornber (1987, fig. 3) developed an

Fig. 7. AFM plots of samples of whole rock lavas (WR), bulk differentiates (D) and residual glasses (G) from three basalts containing
vesicle cylinders; number of analyses are in parentheses. Representative analyses appear in Table 4 and Table 5. The trends parallel
fractional crystallization trends observed in larger basaltic bodies such as lava lakes, sills and layered gabbros.
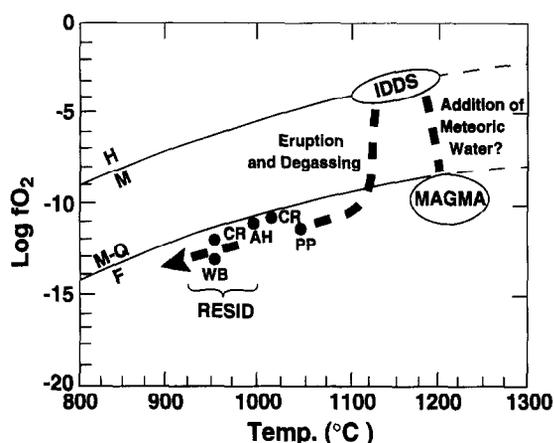
Fig. 8. Plot of f_{O_2} versus temperature for basalts containing vesicle cylinders and high-temperature iddingsite; presence of iddingsite alteration in olivine phenocrysts at eruption requires unusually high f_{O_2}. Possibly, late addition of relatively near surface meteoric water into the magma causes these oxidizing conditions. After eruption, f_{O_2} in lava drops dramatically as volatiles are released. Conditions in the differentiated liquids of vesicle cylinders and sheets parallel the FMQ buffer with falling temperature. Points refer to analyzed Fe-Ti oxide pairs; data screened using test of Bacon and Hirchmann (1988) and reduced with Ca-QUILF (Lindsley and Frost, 1992). AH = Togiak basalt; CR = Crag Rat basalt; PP = Panorama Point basalt; WB = Warner basalt.

empirical method to equate the MgO and CaO contents of Kilauea Iki glasses to temperature. These authors state that the MgO calibration "holds principally for glass coexisting with olivine" and that the

CaO calibration "is valid only for glasses that coexist with olivine + augite + plagioclase...". Although the Kilauea Iki data are not directly comparable to the cylinder-bearing lavas described in Table 4 due to differences in composition (Kilauea lavas have lower Al_2O_3) and differences in initial phenocrysts (Kilauea lavas only have olivine), rough temperature estimates can be evaluated. Quench glasses from the chilled crusts of the flows (i.e., Table 5) cannot be used with either calibration because the glasses coexist with olivine and plagioclase. On the other hand, residual glasses in the differentiates coexist with the three phases satisfying the CaO calibration, thus the indicated formation temperatures are ≤ 1000°C. These values agree with the Fe-Ti oxide temperatures described above.

5. Source of water

Vesicle cylinders form in diktytaxitic basalts that are relatively rich in dissolved volatiles, probably mostly water. Several facts indicate that the cylinders do not form merely because basaltic lavas flow over a wet substrate. First, increasing flow-rock porosity correlates well with increasing groundmass crystal size and increasing population of cylinders (Table 2). Second, vesicle cylinders are commonly found throughout the entire lateral extent of the basalt flows that host them. This observation holds even for

Table 6
Silica and $\delta^{18}O$ analyses of host–differentiate pairs for four vesicle-cylinder-bearing lavas

Description	Sample No.	SiO$_2$ (wt.%) [a]	$\delta^{18}O$ (‰) [b]
Vesicle-cylinder-bearing lavas			
Panorama Point	PP1k (host)	47.6	5.0
	PP1kS (diff.)	47.6	5.2
Underwood	UV2 (host)	~	5.7
	UV1C (diff.)	~	5.0
Togiak	AH26 (host)	50.9	5.4
	AH25S (diff.)	53.6	5.8
Petroglyph	F76-20 (host)	49.5	6.6
	F76-21 (diff.)	50.0	6.3
Typical high-alumina tholeiites [c]	–	48.3–52.8 (n = 11)	6.6 ± 0.6(1σ)

[a] Analyses in Table 1 and Goff (1977).
[b] Analyses by J.R. O'Neil (USGS, 1977).
[c] Data of F. Goff (unpubl.); samples from flows at Mount St. Helens (Washington), Pacaya (Guatemala) and Satsuma Iwo-jima (Japan) volcanoes.

flood basalts like the Museum flow which crops out for many kilometers along the Columbia River near Vantage, Washington and for the Warner Basalt, a plateau basalt found throughout a large sector of northeastern California. Third, flows with vesicle cylinders may overlie any rock type or combination of rock types including other basalt flows. All flows in a vertical stack may contain vesicle cylinders.

It cannot be argued that the cylinders grow by diffusion of water vapor into the flow from underlying rocks, for example, wet sediments, because many flows containing vesicle cylinders overlie rocks that were presumably not water bearing. In addition, most basalt flows extruded over wet sediments do not contain vesicle cylinders. These features indicate that the high water contents that create the cylinders, diktytaxitic textures, and (in some cases) high-temperature iddingsite are inherent to the parent magmas before eruption.

Oxygen isotope analyses were obtained on four pairs of differentiate and host lava (Table 6) to test for addition of relatively shallow (isotopically depleted) meteoric water into magmas that form vesicle cylinders. All host lavas listed in Table 6 are high-alumina basalts. Oxygen isotope values of all samples range from 5.0 to 6.6‰, but no consistent trend is observed in differentiate–host pairs. Because most differentiate samples show chemical enrichment in iron and crystallize significant amounts of magnetite, it might be expected that the $\delta^{18}O$ values of the differentiates would be depleted relative to the host basalts (Hoefs, 1973, p. 57), but this is not necessarily the case.

Interestingly, the lava with the most depleted isotopic composition (5.0‰, Panorama Point basalt) is also the one containing the most intense iddingsite alteration of olivine, the greatest flow porosity, the largest groundmass phenocryst dimensions and the highest abundance of vesicle cylinders (Table 2). Although this basalt has an isotopic composition resembling the most primitive Hawaiian tholeiites (Garcia et al., 1989), it resides in an arc setting where more enriched $\delta^{18}O$ values are commonly found. Typical high-alumina basalts studied by the author from the United States, Guatemala and Japan have $\delta^{18}O$ values $\geq 6.0‰$ (Table 6) but do not contain high-temperature iddingsite or vesicle cylinders. Possibly, the Panorama Point basalt and some

other vesicle cylinder-producing magmas acquire some isotopically depleted meteoric water during their evolution, which contributes to formation of the cylinders and other textural features.

6. Growth of vesicle cylinders

6.1. Time frame of growth

If the cooling history of the lavas and the temperature of formation of vesicle cylinders are known, then the length of time required for the cylinders to grow can be estimated. The approximate cooling history for the Panorama Point basalt is shown in Fig. 9 (Jaeger, 1961). This model assumes pure conductive cooling (thus, maximum cooling time) but is an adequate assumption for the typical flows containing vesicle cylinders. For this example, the cylinders initially form about 50 cm above the flow base at about 1075°C or about 1 day after the flow comes to rest. The cylinders pool into vesiculated pods 1–3 m beneath the flow top. For the chilled crust to become so rigid that differentiate cannot penetrate it requires temperatures approaching the solidus, about 1050°C or less for Hawaiian tholeiite (Shaw et al., 1968; Helz, 1987). Using this value as a minimum temperature of ponding, the cylinders pond
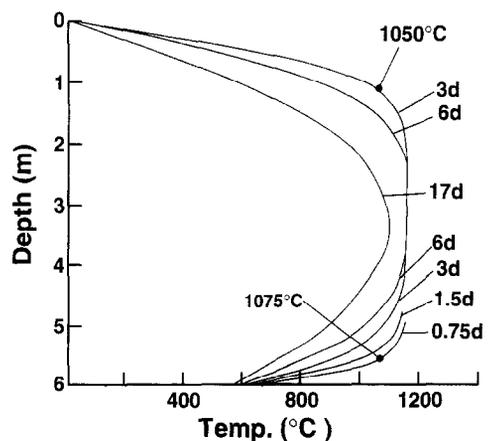

Fig. 9. Temperature versus depth profiles at different times (days) after eruption for a 6-m-thick basalt flow erupting at 1150°C (Jaeger, 1961). The profiles shown emphasize conditions governing the formation of the initial vesicle cylinders; temperatures are discussed in text.

at the base of the chilled crust in 2–3 days after eruption, having risen 4.5 m in about 1.5 day. This gives an average ascent velocity of about 3.5×10^{-3} cm/s.

Raising the temperatures used in this example by 25°C (to 1100 and 1075°C, respectively) does not significantly change this calculation. Increasing the thickness of the flow has a greater impact; for example, if the thickness is 12 m, the mean ascent velocity for the first formed cylinders is approximately doubled. As the flow cools and the chilled crusts at top and bottom increase in thickness, the apparent mean ascent velocity of later formed cylinders decreases. For a 6 m thick flow, no cylinders can grow after about 15 days, because the interior of the flow has cooled to near the solidus.

An interesting check on these time frames and ascent velocities is provided by a calculation of the minimum length of time required to settle out a layer of groundmass olivine in a 8-cm-thick vesicle sheet fed by cylinders in the same flow (Fig. 4b). The average diameter of the iddingsitized olivine crystals is 1 mm and the calculated viscosity of the differentiated liquid in the sheet at 1075°C is $\sim 1 \times 10^4$ poise. Approximate viscosities of silicate liquids can be calculated as functions of temperature from chemical analyses of the liquids (Shaw, 1972). Increased viscosity due to presence of crystals can be estimated using Pinkerton and Stevenson (1992) or a variety of equations in Dingwell et al. (1993). Viscosity changes due to bubbles can be calculated from the Sibree equation (Shaw, 1965) or equations in Dingwell et al. (1993). For this example, values of 0.5 wt.% water, 40% crystals, 10% vesicles, and analysis PP3S (Table 4) were used. The density of olivine, Fo_{80}, at magmatic temperatures is about 3.3 g/cm^3 and the density of the enclosing liquid with 10% vapor bubbles is roughly 2.5 g/cm^3. From the Stokes equation, the terminal velocity of the olivine settling in the liquid is about 3.8×10^{-5} cm/s and the time to fall 8 cm would be ~ 2.4 days. This time is compatible with those shown in Fig. 9.

The calculated settling velocity of the olivine in the vesicle sheet is roughly two orders of magnitude slower than the ascent velocity of liquid in the cylinders. This is consistent with the fact that no layers of olivine or other groundmass minerals are ever found in the cylinders; the crystals are swept into the sheets. Thicker sheets usually show crystal settling textures.

6.2. Viscosity of enclosing lava

The Stokes equation (or refinements, Aubele et al., 1988) can also be used to estimate the bulk viscosity of the lava enclosing the vesicle cylinders during their growth. If the average ascent velocity is $\sim 3 \times 10^{-3}$ cm/s and if we assume that the rising plume of frothy differentiate averages 10 cm in diameter, contains 30% bubbles, and behaves as a coherent mass, then the bulk viscosity of the lava is $\sim 1 \times 10^6$ poise. Viscosity values approaching 10^6 poise require that the static lava has become a mush of crystals, residual melt and small vapor bubbles. This is probably close to an upper viscosity limit because the cylinders are typically 2 cm in diameter near their base and grow by continual addition of residual melt and expanding vapor siphoned from the surrounding crystal-rich, diktytaxitic host (gas filter-pressing, Anderson et al., 1984).

Careful examination of host basalt adjacent to cylinders reveals that the host is commonly drained of residual liquid (Goff, 1977). Vesicle cylinders apparently increase their girth by this process for some time after the plume has ponded beneath the top crust because groundmass plagioclase crystals in coarsely porphyritic flows are aligned around the perimeter of the cylinders. These features indicate that the cylinders expand in the host basalt during growth and that the viscosity of the differentiate is less than the viscosity of the enclosing lava.

Viscosities of the lavas at eruption are much less than values discussed above due to higher temperatures, less crystals, less vapor bubbles and more dissolved water. Calculated eruption viscosities for the lavas listed in Table 2 are about 10^1–10^2 poise using the method of Shaw (1972) and other parameters determined as above.

6.3. Possible growth mechanisms

Field evidence strongly suggests that formation of bubbles in cooling but relatively static, water-rich basalt initiates the growth of vesicle cylinders. Field evidence and the simple calculations above indicate that the frothy differentiate is less viscous and dense

than the host lava when the cylinders grow. Where spacings among cylinders can be observed, they show fairly uniform separations; thus conditions that favor growth of the cylinders are relatively uniform throughout the lateral extent of the flow.

In an earlier study, Goff (1977) proposed that vesicle cylinders may originate from Raleigh–Taylor Instability (RTI) within the lower part of the lava flow. This model requires that a relatively thin horizon or layer of bubble-rich, low-density differentiate develops near the base of the cooling flow and evolves into plumes which rise through the flow to achieve gravitational equilibrium. The potential appeal of this model lies in the fact that low-density
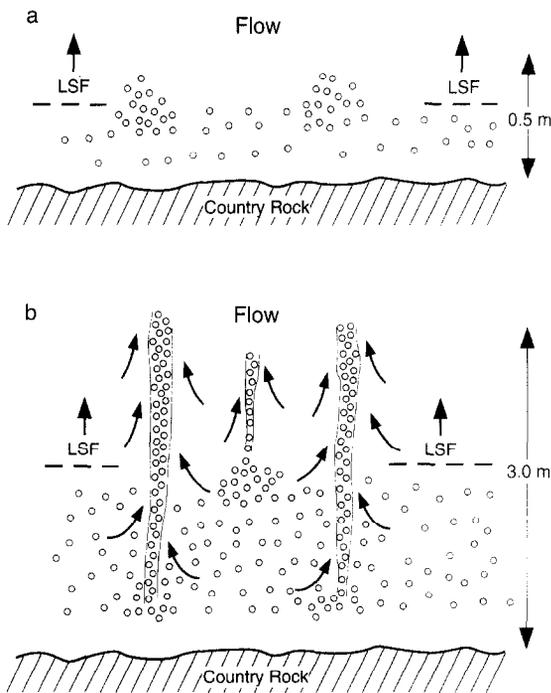

Fig. 10. Cartoons depicting the formation of vesicle cylinders in lavas. (a) Coalescing clusters of bubbles form proto-cylinders (i.e., Fig. 5b) in the lower solidification front (LSF) near the base of the flow (Manga and Stone, 1994). (b) Once a cluster of low-density bubbles begins to rise, residual melt and vapor in the diktytaxitic lava migrate into the low-pressure region created by this disturbance (gas filter-pressing; Anderson et al., 1984). Continued accumulation of vapor and differentiate, and reduced overburden pressure from the enclosing lava cause the cylinders to increase in diameter as they rise toward the chilled upper crust. Upward migration of the solidification front causes new cylinders to begin growth at higher levels in the flow.

plumes and diapirs resulting from RTI have fairly regular spacings (Selig, 1965; Bradley, 1965). A major defect of this model is that there is little evidence that such layers once existed in the flows. Also, the initial conditions of RTI imply that the bubble-rich layers are more viscous than the overlying host basalt (Plesset and Whipple, 1974).

The only other mechanism for growth of vesicle cylinders has been offered by Manga and Stone (1994) who suggest that the cylinders develop from instabilities of bubble concentration. Such instabilities may also occur at fairly regular spacings. These authors have not yet formulated an appropriate model for cylinder growth because they have incorrectly identified the contents of the cylinders as "highly vesicular basalt" and have ignored the chemical and textural features peculiar to vesicle-cylinder-bearing lavas. However, if a small region in the lower part of a diktytaxitic flow accumulates excess bubbles during secondary vesiculation (McMillan et al., 1989), their coalescence and relatively rapid rise might create a vertical, low-pressure discontinuity into which residual liquid and additional vapor would preferentially enter from the enclosing lava (Anderson et al., 1984). Coalescence of bubbles above an upward migrating solidification front is key to initial formation of vesicle cylinders but flowage of differentiated liquid from the vapor-rich host into the plumes is necessary for continued growth (Fig. 10).

7. Discussion

Field relations, petrology and geochemistry of vesicle-cylinder-bearing lavas clearly show that crystal fractionation is occurring by "vapor-differentiation" into low-density, vesicular plumes (Goff, 1977). This mechanism for fractionation is much different than crystal fractionation by gravity settling, the most common type, although chemical and mineralogical trends are similar. "Vapor-fractionation" is a similar term that has been used to describe very different kinds of processes, such as chemical variations in certain rock suites (Smyth, 1913) and volatile transport of chemical and mineral species in a variety of environments (Fenner, 1926). In his initial study of the Hat Creek Basalt, Anderson (1971, p. 300) recognized that "vapor transport"

had somehow caused residual glasses to form linings and oozes in pre-existing vesicles and near-surface fractures. However, Anderson also suggested that much of the chemical fractionation in the differentiates was caused by transport of major and minor elements in a gas phase. Anderson et al. (1984) later coined the term "gas filter-pressing" for the process during which "residual liquid migrates through a porous and permeable, but rigid, network of interlocking crystals in response to a pressure gradient generated by vapor-saturated crystallization". This process occurs as residual melt and volatiles migrate into vesicle cylinders; thus "vapor-differentiation" and "gas filter-pressing" are terms with essentially identical meanings in the small-scale sense.

The one-to-one association of vesicle cylinders with lavas having diktytaxitic textures is fundamental to an understanding of the root cause of vapor-differentiated basalt flows described herein. Phenocryst textures, lava porosities, cylinder densities and other features suggest that higher than normal water contents characterize the parent magmas. The high water content of many high-alumina tholeiites was noted previously by Anderson (1973) but diktytaxitic textures and vesicle cylinders are not restricted to high-alumina tholeiites (Table 1).

High-temperature iddingsite alteration of olivine phenocrysts, which is found in many vesicle-cylinder-bearing lavas, is another indication of high water contents in the parent magmas. High water contents can promote oxidation of iron-bearing phases. The iddingsite contains a high-temperature iron-oxide phase (γ-Fe_2O_3). Textures show that the oxidation of the olivine commonly occurs before eruption (requiring high f_{O_2} in the magma before eruption). Since the oxidation affects only the outer margins and fractures cutting the phenocrysts, the oxidation (and input of additional water?) appear to happen at a late stage in the evolution of the magma.

An important unresolved issue is to determine the quantity and source of water in the diktytaxitic lavas that produce vesicle cylinders and associated structures. Accurate pre-eruption water contents can be determined by analysis of glass inclusions and can be estimated by means of experimental methods such as plagioclase–melt equilibria (Housh and Luhr, 1991). Sources of water might be determined by analyzing the oxygen isotopes of many more host–

differentiate pairs or by using laser isotope techniques to study the phenocryst and groundmass compositions of the lavas and the composition of the high-temperature iddingsite. Late (meteoric) water addition should produce depleted oxygen isotope compositions in the iddingsite relative to the phenocryst phases unless magmatic temperatures cause extremely rapid re-equilibration of the isotopes.

Because diktytaxitic lavas containing vesicle cylinders and high-temperature iddingsite are relatively widespread and are not restricted by age, tectonic style, or chemical type, a deep source for the high water contents has interesting implications on generation of basaltic magmas. If the source is relatively shallow, meteoric water is more easily assimilated into basaltic magmas than many geologists realize. Magma generation and ascent are such complicated processes that there may be no unique source for all basalts.

8. Conclusions

Well-developed vesicle cylinders form only in diktytaxitic basalt flows and are composed of low-density, vertical plumes of bubble-rich differentiated liquid. Flows containing vesicle cylinders display pahoe-hoe surfaces and other features indicative of relatively high eruption temperatures and low eruption viscosities. Field observations and textural evidence observed in cylinder-bearing flows also show that the host lavas contained unusually high water contents. Paragenetic mineral and geochemical trends from enclosing lava to cylinder differentiates to residual glasses parallel classic fractional crystallization trends observed in larger basaltic bodies such as lava lakes, diabase sills and layered gabbros. Gravity settling of early formed mineral phases is the major cause of crystal fractionation in these larger bodies whereas vapor differentiation is the cause of fractionation in cylinder-bearing flows.

Mineral compositions and paragenesis for the high-temperature iddingsite and Fe-Ti oxides imply that the f_{O_2} of many cylinder-bearing lavas was extremely high before eruption ($\sim 10^{-4}$) and dropped abruptly after eruption ($\sim 10^{-11}$). Oxygen-18 results suggest that cylinder-bearing lavas are slightly depleted compared to compositionally simi-

lar lavas without vesicle cylinders, although this apparent depletion requires further substantiation. Because the iddingsite described herein forms before eruption, the evidence suggests that basaltic magmas producing vesicle cylinders gain meteoric water late in their evolution. Determination of the source of water (shallow or deep) is of fundamental interest because diktytaxitic lavas are common in arc, rift and flood basalt environments.

Field relations limit the time of formation of vesicle cylinders to the period between the cessation of lava movement and deep penetration of columnar joints. Simple conductive cooling models place the growth period of the cylinders at 1–5 days after basalt flows of typical thickness (3–10 m) come to rest. Stokes equation calculations suggest that the host lavas have viscosities as high as 10^6 poise when the cylinders rise. In contrast, the frothy differentiates filling vesicle cylinders have calculated viscosities of around 10^4 poise.

Growth of vesicle cylinders is apparently triggered by density instabilities that develop when the host basalt forms zones of coalesced bubbles above the lower solidification front of the flow during secondary vesiculation. Once these coalesced bubbles begin to rise, they form a low-pressure, vertical discontinuity into which residual liquid and additional vapor enters by gas filter-pressing. However, a quantitative model that combines all observations and predicts parameters, such as mean spacing between cylinders, has not yet been formulated.

Acknowledgements

References

Anderson, A.T., 1971. Alkali-rich, SiO_2 deficient glasses in high-alumina olivine tholeiite, Hat Creek Valley, California. Am. J. Sci., 271: 293–303.

Anderson, A.T., 1973. The before-eruption water content of some high alumina magmas. Bull. Volcanol., 37(4): 530–552.

Anderson, A.T. and Gottfried, D., 1971. Contrasting behavior of P, Ti, and Nb in a differentiated high-alumina tholeiite and a calc-alkaline andesite suite. Geol. Soc. Am. Bull., 82: 1929–1942.

Anderson, A.T., Swihart, G.H., Artioli, G. and Geiger, C.A., 1984. Segregation vesicles, gas filter-pressing, and igneous differentiation. J. Geol., 92: 55–72.

Aubele, J.C., Crumpler, L.S. and Elston, W.E., 1988. Vesicle zonation and vertical structure of basalt flows. J. Volcanol. Geotherm. Res., 35: 349–374.

Bacon, C.R. and Hirchmann, M.M., 1988. Mg/Mn partitioning as a test for equilibrium between coexisting Fe-Ti oxides. Am. Mineral., 73: 57–61.

Bowen, N.L., 1928. The Evolution of the Igneous Rocks. Princeton Univ. Press, Princeton, NJ, 332 pp.

Bradley, W.H., 1965. Vertical density currents. Science, 150: 1423–1428.

Champness, P.E., 1970. Nucleation and growth of iron oxides in olivines, $(Mg,Fe)_2SiO_4$. Mineral. Mag., 37: 790–800.

Chapman, M. and Rhodes, J.M., 1992. Composite layering in the Isle au Haut igneous complex, Maine: Evidence for periodic invasion of a mafic magma into an evolving magma reservoir. J. Volcanol. Geotherm. Res., 51: 41–60.

Cornwall, H.R., 1951. Diffrentiation in lavas of the Keweenawan series and the origin of the copper deposits of Michigan. Geol. Soc. Am. Bull., 62: 159–202.

Dingwell, D.B., Bagdassarov, N.S., Bussod, G.Y. and Webb, S.L., 1993. Magma rheology. Mineral. Assoc. Can., Short Course, 21: 131–196.

Fenner, C.N., 1926. The Katmai magmatic province. J. Geol., 35: 673–770.

Fuller, R.E., 1931. The geomorphology and volcanic sequence of Steens Mountain in southeastern Oregon. Univ. Washington, Publ. Geol., 3: 1–130.

Garcia, M.O., Muenow, D.W., Aggrey, K.E. and O'Neil, J.R., 1989. Major element, volatile, and stable isotope geochemistry of Hawaiian submarine tholeiitic glasses. J. Geophys. Res., 94: 10,525–10,538.

Goff, F.E., 1977. Vesicle cylinders in vapor-differentiated basalt flows. Ph.D. Thesis, Univ. California, Santa Cruz, CA, 181 pp.

Goff, F., 1995. Vesicle cylinders in the Warner and Hat Creek Basalts, northeastern California. Friends of the Pleistocene, Fall 1995 Field Trip Guideb., 10 pp.

Goode, A.D.T., 1974. Oxidation of natural olivines. Nature, 248: 500–501.

Haggerty, E.S. and Baker, I., 1967. The alteration of olivine in basaltic and associated lavas: Part I. High-temperature alteration. Contrib. Mineral. Petrol., 16: 233–257.

Helz, R.T., 1980. Crystallization history of Kilauea Iki lava lake as seen in drill core recovered in 1967–1979. Bull. Volcanol., 43: 675–701.

Helz, R.T., 1987. Differentiation behavior of Kilauea Iki lava lake, Hawaii: An overview of past and current work. In: Magmatic Processes: Physicochemical Principals. Geochem. Soc. Spec. Publ., 1: 241–258.

Helz, R.T. and Thornber, C.R., 1987. Geothermometry of Kilauea Iki lava lake, Hawaii. Bull. Volcanol., 49: 651–668.

Hiza, M., 1988. Characteristics of vesicular segregations in the Switzer Mesa Basalt, northern Arizona. Annu. Symp. Geol. Paleontol., Museum of Northern Arizona, Flagstaff, AZ, 1 p. (abstract).

Hoefs, J., 1973. Stable Isotope Geochemistry. Springer, New York, NY, 140 pp.

Hon, K., Kauahikaua, J., Delinger, R. and Mackay, K., 1994. Emplacement and inflation of pahoehoe sheet flows: Observations and measurements of active lava flows on Kilauea volcano, Hawaii. Geol. Soc. Am. Bull., 106: 351–370.

Housh, T.B. and Luhr, J.F., 1991. Plagioclase-melt equilibria in hydrous systems. Am. Mineral., 76: 477–492.

Jaeger, J.C., 1961. The cooling of irregularly shaped igneous bodies. Am. J. Sci., 259: 721–734.

Kuno, H., 1965. Fractionation trends of basalt magmas in lava flows. J. Petrol., 6: 302–321.

Lindsley, D.H. and Frost, B.R., 1992. Equilibria among Fe-Ti oxides, pyroxenes, olivine, and quartz: Part I. Theory. Am. Mineral., 77: 987–1003.

Manga, M. and Stone, H.A., 1994. Interactions between bubbles in magmas and lavas: Effects of bubble deformation. J. Volcanol. Geotherm. Res., 63: 267–279.

McMillan, K., Long, P.E. and Cross, R.C., 1989. Vesiculation in Columbia River basalts. In: S.P. Reidel and P.R. Hooper (Editors), Volcanism and Tectonism in the Columbia River Flood-Basalt Province. Geol. Soc. Am. Spec. Pap., 239: 157–167.

Murata, K.J. and Richter, D.H., 1961. Magmatic differentiation in the Uwekahuma Laccolith, Kilauea Caldera, Hawaii. J. Petrol., 2: 424–437.

Philpotts, A.R. and Lewis, C.L., 1987. Pipe vesicles—An alternate model for their origin. Geology, 15: 971–974.

Pinkerton, H. and Stevenson, R.J., 1992. Methods of determining the rheological properties of magmas at sub-liquidus temperature. J. Volcanol. Geotherm. Res., 53: 47–66.

Plesset, M.S. and Whipple, C.G., 1974. Viscous effects in Rayleigh–Taylor instability. Phys. Fluids, 17: 1–17.

Roeder, P.L. and Emslie, R.F., 1970. Olivine–liquid equilibrium. Contrib. Mineral. Petrol., 29: 275–289.

Russell, J.K. and Stanley, C.R. (Editors), 1990. Theory and application of Pearce element ratios to geochemical data analysis. Geol. Assoc. Can. Short Course 8, 315 pp.

Selig, F., 1965. A theoretical prediction of salt dome patterns. Geophysica, 20: 633–644.

Shaw, H.R., 1965. Comments on viscosity, crystal settling, and convection in granitic magmas. Am. J. Sci., 263: 120–152.

Shaw, H.R., 1972. Viscosities of magmatic silicate liquids: An empirical method of prediction. Am. J. Sci., 272: 870–893.

Shaw, H.R., Peck, D.L., Wright, T.L. and Okamura, R., 1968. The viscosity of basaltic magma: An analysis of field measurements in Makaopuhi Lava Lake, Hawaii. Am. J. Sci., 266: 225–264.

Smyth, C.H., 1913. The chemical composition of the alkaline rocks and its significance as to their origin. Am. J. Sci., Ser. 4, 36: 33–46.

Wager, L.R., 1960. The major element variation of the layered series of the Skaergaard Intrusion and a re-estimation of the average composition of the hidden layered series and of the successive residual magmas. J. Petrol., 1: 364–398.

Walker, F., 1956. The magnetic properties and differentiation of dolerite sills—A critical discussion. Am. J. Sci., 254: 433–451.